IEEE Access
Multidisciplinary | Rapid Review | Open Access Journal

Received July 26, 2019, accepted August 17, 2019, date of publication August 22, 2019, date of current version September 5, 2019.

Digital Object Identifier 10.1109/ACCESS.2019.2936892

Diagnosis of Plant Cold Damage Based on Hyperspectral Imaging and Convolutional Neural Network

WEI YANG[1], CE YANG[2], ZIYUAN HAO[1], CHUANQI XIE[3], AND MINZAN LI[1]

[1]Key Laboratory of Modern Precision Agriculture System Integration Research, China Agricultural University, Beijing 100083, China
[2]Department of Bioproducts and Biosystems Engineering, University of Minnesota, Twin Cities, Saint Paul, MN 55108, USA
[3]Department of Food Science and Engineering, East China University of Science and Technology, Shanghai 200237, China

Corresponding author: Ce Yang (ceyang@umn.edu)

This work was supported in part by the Chinese National Key Research and Development Plan under Grant 2016YFD0700300-2016YFD0700304, in part by the Basic Research Funding of the China Agricultural University under Grant 2019TC049, and in part by the MNDrive Robotics, Sensors and Advanced Manufacturing Initiative at the University of Minnesota.

ABSTRACT Cold damage is one of the disasters that cause significant loss and irreversible damage in crop production. To avoid yield loss, high-throughput phenotyping can be used to select the crop varieties with cold stress resistance. Nowadays, non-destructive spectral image analysis has become an effective way and is widely used in high-throughput phenotyping, which reflects the structural, physiological, biochemical characteristics and traits of plant structure and composition, plant growth and development processes and outcomes. This study used convolutional neural network (CNN) model to extract spectral features in the visible-near-infrared range to estimate cold damage of corn seedlings. The hyperspectral images of cold treated corn seedlings from five varieties were used as research objects in this study. The spectral range of the images was 450-885nm. Gaussian low-pass filter and the Savitzky-Golay smoothing method combined with the first-order derivative was used to do pre-processing for spectral data. For each corn variety, 3600 pixel samples obtained from the selected region of interests in each variety of corn seedlings were used for the CNN modeling. After the CNN modeling, 400 pixel samples extracted from the hyperspectral images were used as the testing set for each variety. Finally, a 10-layer knot CNN model was determined by analyzing the classification accuracy and computational efficiency. CNN detected the cold damage level of different types of corn seedlings as W22 (41.8 %), BxM (35%), B73 (25.6%), PH207 (20%), Mo17 (14%), which had high correlation with the ranking given by chemical method. The coefficient of correlation between cold damage detection results of CNN and results from chemical method is 0.8219. Therefore, it proves that spectral analysis based on CNN modeling can provide reference for detecting cold damage in corn seedlings.

INDEX TERMS CNN, deep learning, cold damage, hyperspectral imaging, high-throughput phenotyping, corn.

I. INTRODUCTION

Cold damage refers to the phenomenon that crops delay or stop growing when the temperature drops below the temperature limit during the growth of crops. When crops suffer from low temperatures, the disaster is called cold damage. Cold damage occurs mostly in the fall-winter transition and winter-spring transition. It is often a short-term low-temperature disaster. There have been many reports in cold damage researches. Some researchers have made progress on the mechanism and defense measures of cold damage, but real-time monitoring of cold damage is still very limited [1], [2]. The traditional method of cold damage diagnosis is mainly carried out through field investigation and temperature data evaluation, which are time-consuming and laborious. In many cases, remote sensing methods were able to provide the detailed, rapid and wide-range understanding of disasters [3], [4]. Therefore, remote sensing-based diagnostic methods are receiving increasing attention. In recent years, these methods can be roughly divided into three categories: ground minimum temperature inversion, vegetation index difference method and hyperspectral imaging [5]–[8]. Ground minimum temperature inversion is a method derived from the disaster factors caused by cold damage.

The associate editor coordinating the review of this article and approving it for publication was Ruqiang Yan.

Kerdiles established a linear regression relationship between the NOAA-AVHRR brightness temperature data and the lowest temperature data from meteorological stations and carried out research on the spatial mapping of cold damage in winter wheat in Argentina [9]. Juan proposed a universal single window algorithm, which is suitable for surface temperature inversion of a variety of thermal infrared sensors [10]. Vegetation index method is comparing the changes of vegetation index caused by the decrease of crop activity before and after cold damage and then judging the degree of disaster. Jurgens used the Landsat-5TM image to create a T-corrected normalized vegetation index to monitor the cold damage in agriculture [11]. Feng et. al. monitored the cold damage range based on MODIS-NDVI before and after winter wheat cold damage and evaluated the cold damage degree by analyzing the correlation between NDVI recovery rate and winter wheat yield [12]. Omanov studied the cold damage of winter crops in Ukraine by monitoring snow cover and ground temperature using NOAA and MODIS data [13]. Compared to the above methods, the hyperspectral imaging method can accurately monitor physiological state changes, as well as obtain data quickly and accurately. The technical advantages of hyperspectral diagnosis have gradually made it a popular technique in the current cold damage researches. Li Junling et. al. analyzed the correlation between the spectral reflectance data and the chlorophyll content of the leaves before and after cold damage and obtained the characteristic bands for monitoring the cold damage [14]. Wei Chenyang et al. obtained the field experiment of different frost damage treatment of winter wheat, and obtaining many types of hyperspectral parameters in frost temperature and combined with winter wheat yield factors, constructed an early spectral diagnostic model for winter wheat night frost damage [15]. Wang et. al. analyzed the smoothed canopy spectral reflectance data of winter wheat and obtained the winter wheat freeze damage severity model with high precision [16]. However, these studies did not utilize the full spectral dimension of the hyperspectral images they collected. In addition, few studies have been done on cold damage discrimination for corn using hyperspectral imaging.

In 2016, Minnesota harvested 8.39 million acres of corn, including 8 million acres of corn grain and 0.39 million acres of corn silage, which directly produced $5.1 billion profit [17]. The corn crops in Minnesota are usually planted in late April or early May. However, the cold weather in May exposes risk to the young seedlings. The abrupt change of temperature will directly affect the corn seedlings. It can delay the development of the maize plants, reduce the number of leaves per plant, decrease the ear counts, reduce the number of grains per ear, and reduce yield by 12%-15% potentially [18]. Thus, non-destructive detection of cold damage could contribute to the increase of profit for farmers in Minnesota.

To detect cold damage using hyperspectral image analysis, multiple neural network algorithms can be applied. The traditional BP neural network propagation has a simple structure with three layers. But it is prone to problems such as inability to converge and easy to fall into local minimum points. Deep learning proposes a method for the computer to automatically learn the characteristics of the pattern and integrates the feature learning into the process of building the model, thus reducing the incompleteness caused by the artificial design features. Deep learning is different from traditional artificial neural network-based feature extraction, it automatically extracts features from low-level to high-level layers according to its own architecture. CNN is the most representative method, which has high robustness and strong generalization ability and has been widely used in research fields such as image recognition and machine vision.

Huang et. al. improved the training model based on the GoogLeNet model and cascaded the extracted spike lesions at various scales [19]. They achieved an accuracy rate of 92.0% based on Softmax classification. Liu et. al. enhanced the original image through the feature map, then down sampled the recommended region through RPN and carried out border regression and classification [20]. The detection rate of the grape disease was 87.2%. Liu et. al. combined the sparse self-encoder and CNN to increase the network branch, and the sample input from the encoder training to obtain the low-dimensional features representing the initial weight of the CNN, which not only solved its own small sample size problem but also accelerated the convergence of the network [21]. Tan proposed a feature recognition method for elastic momentum deep convolution lesions. Weight-update mechanism of elastic impulses was proposed based on the back propagation characteristics. He constructed the linear elastic momentum and quadratic elastic momentum. The integrated learning network fusion of feature extraction and pattern recognition speeded up the convergence [22].

Therefore, this paper aims to study the corn seedlings based on hyperspectral imagery after cold stress, extract the spectral curves of the comprehensive evaluation index of cold damage, and use deep learning analysis to construct a model for corn seedling damage detection. It provides theoretical and technical support for real-time monitoring and evaluation of corn seedling cold damage.

II. MATERIALS AND METHODS

A. HYPERSPECTRAL IMAGING SYSTEM

A push broom hyperspectral camera (PIKA II, Resonon, Inc., Bozeman, MT 59715, USA) was used for image collection that required constant relative movement during image acquisition. Normally, a hyperspectral imaging system has two motion control methods: the camera is fixed while the sample is moving, or the sample is fixed while the camera is moving. The latter method was used in this study. The camera was mounted on a linear gear slider and a Dayton DC gear motor (model: 2L008, Dayton electric Mfg Co. Lake Forest, IL 60045, USA) was used to move the slider along at a set speed, with the camera nadir oriented. The structure is shown in Figure 1. All samples were scanned by the hyperspectral

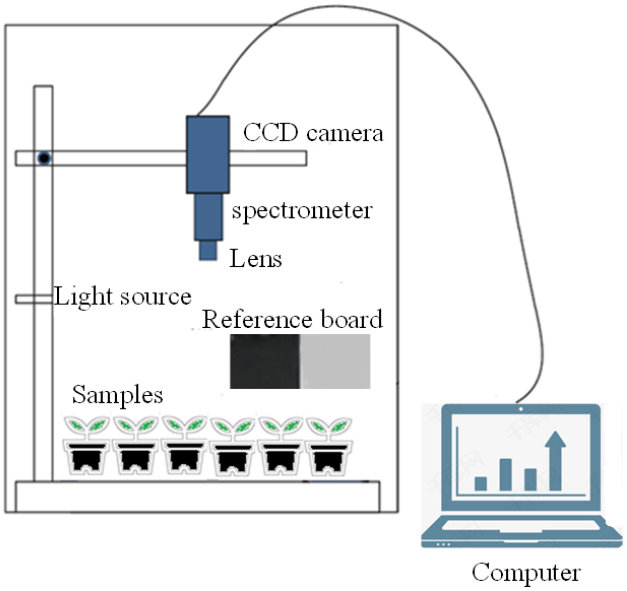

FIGURE 1. The whole structure of the imaging system.

camera line by line. The parameters for the imaging system are as follows:

Spectral range: 395-885 nm
Spectral resolution: 2.05 nm
Spectral bands: 240
Frame rate: 34.0 Hz
Integration time (exposure time): 6.5 ms
Gain: 23.0 dB

B. PLANT SAMPLES

There are two replicate sets (three plants per set) for cold-stressed and control corn plants of five different genotypes. Therefore, a total of 10 hyperspectral images were collected, and each contains six plants (three controls and three cold stressed). The details of the hyperspectral images can be seen in Table 1. '7°C stress day 11' means the plants were grown in the control condition until day 11, and then they were put into a 7°C environment for 8 hours. After that, they were returned to the control condition [18].

C. IMAGE COLLECTION AND CALIBRATION

In this study, a white Teflon reference panel with the spectral reflectance of 99% was taken with the sample in each image. The dark reference image with the spectral reflectance of near 0% was obtained by covering the camera lens and turning off the lights. And the corrected image can be calculated according to Equation (1), which is the empirical calibration method.

$$I_{calibrate} = \frac{I_{original} - I_{dark}}{I_{white} - I_{dark}} \quad (1)$$

where $I_{calibrate}$ is the calibrated image, $I_{original}$ is the original image, I_{white} is the white reference image, and I_{dark} is the dark reference image.

TABLE 1. Details of the samples used in this study.

Genotype	Treatment	HSI picture number
B73	Control	Pic1
	7°C stress day 11	
B73	Control	Pic2
	7°C stress day 11	
Mo17	Control	Pic3
	7°C stress day 11	
Mo17	Control	Pic4
	7°C stress day 11	
BxM	Control	Pic5
	7°C stress day 11	
BxM	Control	Pic6
	7°C stress day 11	
PH207	Control	Pic7
	7°C stress day 11	
PH207	Control	Pic8
	7°C stress day 11	
W22	Control	Pic9
	7°C stress day 11	
W22	Control	Pic10
	7°C stress day 11	

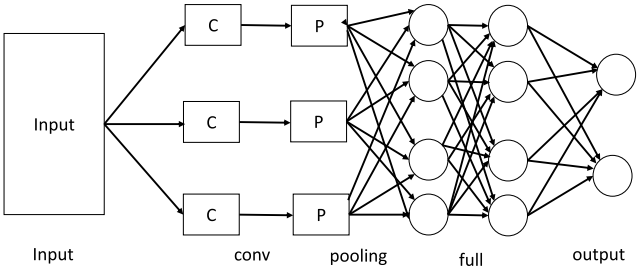

FIGURE 2. The whole structure of the CNN model.

D. DETECTION MODEL

Usually, the deep learning model is initialized by unsupervised learning and builds a multi-layer neural network containing different levels of data representation. The model will be fine-tuned in a supervised way. This structure can learn from the shallow representation of the more essential deep features, which are useful for extracting the abstract features and invariant features of the data. CNN gives better results in terms of image and speech recognition than other deep learning structures. Compared to other depth and feedforward neural networks, CNN requires fewer parameters which make it a more suitable deep learning structure for the cold damage detection using hyperspectral imaging.

CNN is a feedforward neural network, which is especially prominent in the field of image recognition research. The basic architecture of the network usually consists of three types of layers: convolution layers, pooling layers, and fully connected layers. A batch normalization algorithm is also used, which normalizes the input of each layer to ensure that the input data distribution of each layer is stable, thereby accelerating the training. In the process of network training, the parameter update will cause the distribution of input data of each layer of the network to change constantly. Then each layer needs to be constantly changed in the process of training to adapt to this new data distribution, so the final e structure of the CNN need a training process. Figure 2 is the structure

of the CNN model. The purpose of the convolution layer is to continuously learn the input sample features. As shown in Figure 6, the convolution layer consists of several feature maps. Each neuron of a feature map is connected to a neuron on its upper feature map. When a well-conceived convolution kernel (filter) is convolved, a graph is generated. Then, the new data will be passed to a nonlinear activation function, and a new feature map will be obtained by applying convolution kernels. The pooling layer is designed to control the spatial information of the data. The main method is to reduce the resolution of the feature map. The pooling layer is normally located between two convolution layers. After the input data passes several convolutional and pooling layers, one or more fully connected layers will be set. The fully connected layer acts as a ''classifier'' throughout the network. CNN is a shared weight local connected neural network. The neurons from the upper layer only sparsely connected to the neurons from the lower layer and some neurons can share weights and biases. This can reduce the number of training parameters and simplify the network structure as much as possible while extracting more abstract features.

In this study, Softmax Regression is used as it can generate a well-formed probability distribution of the output. Assume a given training set is $\{(x^{(i)}, y^{(i)}); i \in 1, \ldots, N, y^{(i)} \in 0, \ldots, k-1\}$, where $x^{(i)}$ is the i-th input, y(i) is its class label, N is the number of inputs, and k is the number of classes. Then the prediction value $a_j^{(i)}$, which indicates that $x^{(i)}$ belongs to the predicted class j, can be converted with the following Softmax function. Softmax converts the prediction p_j^i to a non-negative value and performs regularization

$$p_j^i = \frac{e^{a_j(i)}}{\sum_{j=0}^{k-1} e^{a_j(i)}} \tag{2}$$

E. DATA PROCESSING

ENVI 4.8 (Research System Inc., USA), MATLAB 7.1 (USA) and Excel 2013 (Microsoft, USA) software was used for data processing. The data processing flowchart is shown in Figure 3. First, we obtained maize seeding hyperspectral images including normal maize seeding and cold-treated maize seeding. The dark current and white boards were used for hyperspectral image calibration. The third step was to split the regions of interest (ROIs) from the hyperspectral images and extract the full spectrum of ROIs. 3600 pixel samples obtained from the region of interests in each corn seedling hyperspectral images were used for the CNN modeling. After obtaining the CNN model, 400 new pixel samples from the hyperspectral images were used as the testing sets, respectively. And then the structure of the CNN model was determined according to the training procedure.

Reflectance curves (sample data) of the pre-treated spectral data were extracted from the hyperspectral images. The method is as follows: The reflectance values were generated by ENVI software. The ROIs are delimited from the images, and then three sample points were extracted from each ROI. The average spectral curve of the three sample data points was

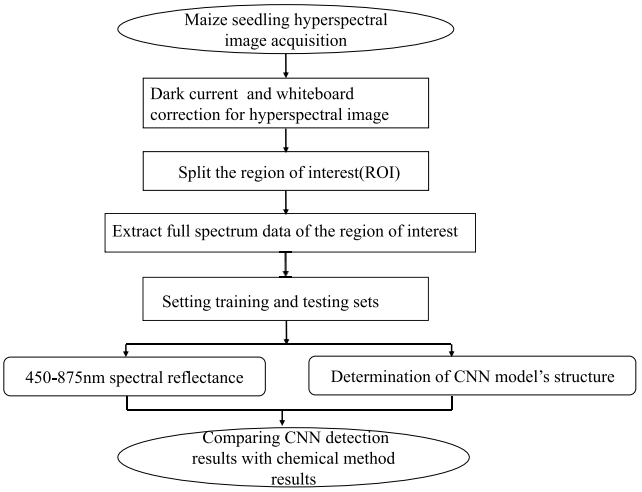

FIGURE 3. The specific data processing process of the paper.

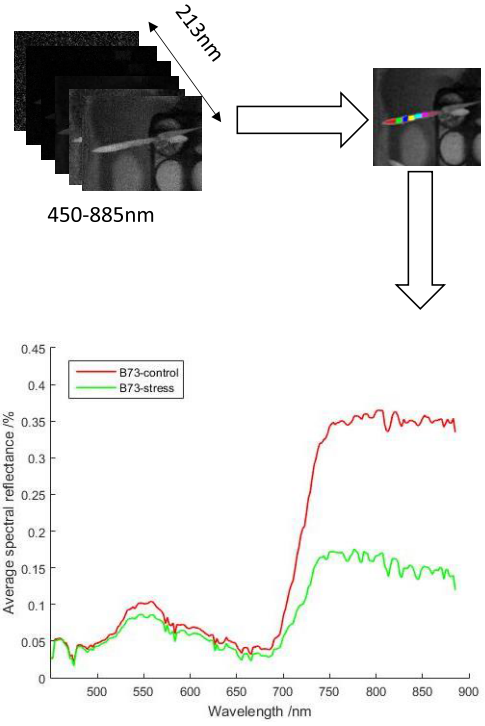

FIGURE 4. The procedure of the sample data selection from ROIs.

used as the representative spectrum of the ROI. Wavelengths 450-885nm (a total of 213 bands) were analyzed due to the noise removal in the 400-450nm range. Figure 4 shows the procedure of the sample data selection. The training set was assigned as shown in Table 2 [26]–[28].

III. ANALYSIS

In order to show the cold damage of different maize genotypes more intuitively, the reflectance curves of the samples were drawn by Matlab and shown in Figure 5. Samples from different corn varieties and treatments are clustered

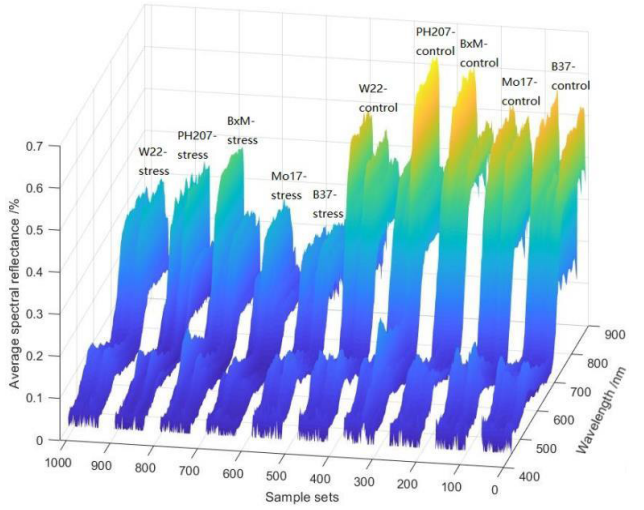

FIGURE 5. 3D spectral plot of the sample.

TABLE 2. Details of the samples used in this study.

Cultivars	Treatments	Training Sample Size
B73	Control	1800
	7°C stress day 11	1800
	Total	3600
Mo17	Control	1800
	7°C stress day 11	1800
	Total	3600
BxM	Control	1800
	7°C stress day 11	1800
	Total	3600
PH207	Control	1800
	7°C stress day 11	1800
	Total	3600
W22	Control	2300
	7°C stress day 11	1300
	Total	3600
Sum	Control	9500
	7°C stress day 11	8500
	Total	18000

and separated by spaces in the x-axis. It can be seen from Figure 5 that the spectral curves of different kinds of samples are similar in pattern, and the wavelengths corresponding to the reflectance peaks have very similar values. For all genotypes, the spectral reflectance values of stressed plants were always lower compared to the control samples. All in all, the specificity of the leaves can be reflected in the spectral domain by hyperspectral techniques [29]–[31]. However, the differences between the control and cold-treated seedlings vary among genotypes, especially in the range of 700-885 nm.

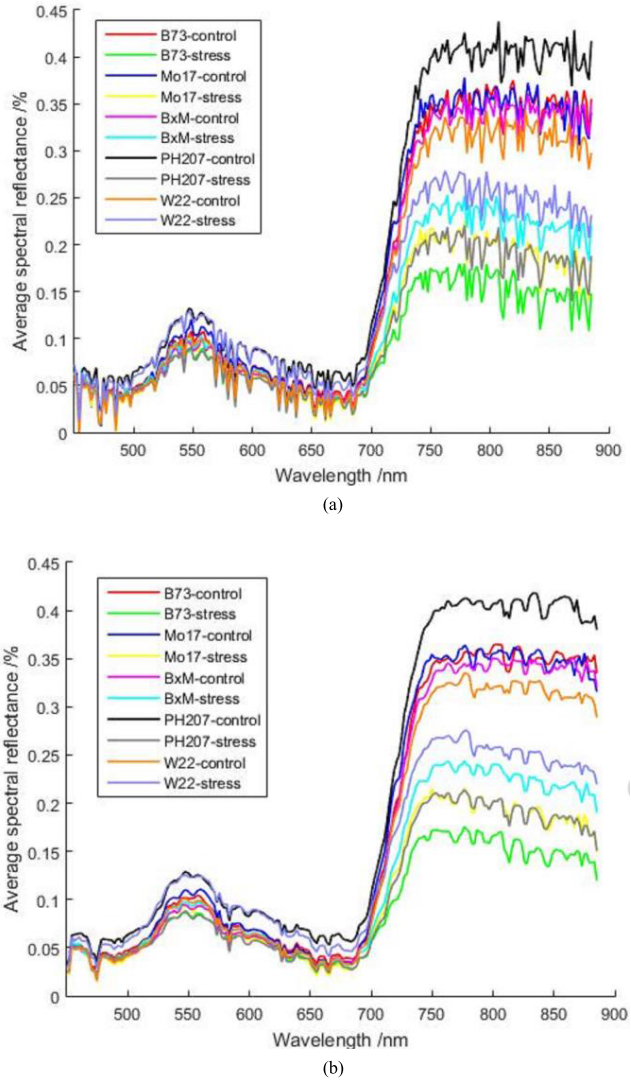

FIGURE 6. The pre-processing result compared with the original data. (a)Original spectral data for corn seeding from five varieties (b) The pre-processing result based on savitzky-golay smoothing method combined with first-order derivative.

The original spectral data points collected from the ROIs contain a variety of noise due to the influence of light source and optical components performance, which will affect the image quality. Therefore, the pre-treatment process is very important for establishing the classification models. Gaussian low-pass filter and the Savitzky-Golay smoothing method combined with the first-order derivative were used to do pre-processing. Gaussian low-pass filter was used to remove noise and then the Savitzky-Golay smoothing method combined with the first-order derivative was used to eliminate the influence of high-frequency noise and baseline offset [23]–[25]. The moving window width of the Savitzky-Golay smoothing method was set to 7 to achieve a better result. With the pre-processing, the average spectral curves for control and cold stressed samples of different genotypes can be seen more clearly in Figure 6-b. For the same genotype, the spectral reflectance values differed between

the control and stressed samples in the near-infrared (NIR) spectral region. The control samples have higher reflectance values than stressed ones in this area. However, W22 has the least spectral differences between the control and stressed samples, which indicates strong cold resistance. There is a spectral peak at 550nm, which is the nitrogen response. In the red edge range (680-710 nm), the spectral reflectance increased sharply. According to a previous study, the low reflectance at 450-680 nm is caused by the strong absorption of photoactive pigments (chlorophylls, anthocyanin and carotenoids), and the high reflectance in the near-infrared range (700-885 nm) is because of the multiple scattering by crop leaf cells. The cold-damaged leaf cells tend to have much lower reflectance in this range.

IV. RESULTS AND DISCUSSIONS

A. THE TRAINING PROCESS OF THE CNN MODEL

In this study, the CNN model was implemented using the Keras framework. Keras is based on the Python language, which enables more efficient optimization, tuning and evaluation of the deep neural networks. The model takes the reflection spectra of corn seedlings as the input and the cold damage level as the output. The following steps were used for the training of the CNN model:

a. Model parameters initiation: initial model parameters θ were randomized, and sample size, the number of training iterations, the learning rate were set to meet the training requirement. In this study, CNN adopts a sequential model. The convolution layer is used for neighborhood filtering on the input spectral signals, the pooling layer performs maximum pooling on the signals.

b. The spectral data input was transformed into a feature sequence after the CNN layers, and the classification decisions were made by the logistic regression classifier. Use x^l as the output of the current layer l, and then calculate: $x^l = f\left(u^l\right)$, where

$$u^l = W^l x^{l-1} + b^l \tag{3}$$

where: W^l and b^l represent the weight and offset of the current layer; f is the layer l's excitation function.

The modified linear unit (ReLU), a non-linear function that allows the network to learn faster and avoids saturation for large positive inputs [32]–[35], was used as the excitation function for the convolution pooling layers and the fully connected layers. The formula of ReLU is:

$$\mathrm{f(x)} = \max(0, \mathrm{x}) \tag{4}$$

Compared with sigmoid and tanh, the advantage of ReLU is:

(1)The gradient is not saturated. The gradient calculation formula is: $1\{\mathrm{X} > 0\}$. Therefore, in the back propagation process, the problem of gradient dispersion is alleviated, and the parameters of the first few layers of the neural network can be quickly updated.

(2) The calculation speed is fast. During forward propagation, the sigmoid and tanh functions need to calculate the exponent when calculating the activation value, while the ReLU function only needs to set the threshold. If $\mathrm{x} < 0$, $\mathrm{f(x)} = 0$, if $\mathrm{x} > 0$, $\mathrm{f(x)} = \mathrm{x}$. Speed up the calculation of forward propagation. Therefore, the ReLU activation function can greatly speed up the convergence.

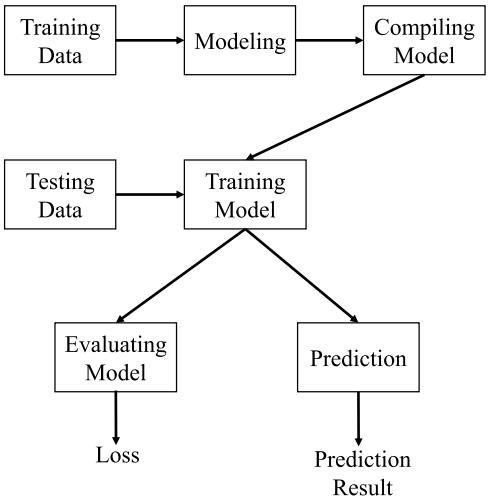

FIGURE 7. The training process.

The pooling layer uses the maximization function maximum, the output layer uses the softmax function and outputs the classification label, and P(y) predicts the probability of belonging to each class in the current iteration. The calculation formula is as follows

$$\mathrm{P}(y = l|x, W, b) = s(Wx + b) = \frac{\exp\left(W_i^T x_i + b_i\right)}{\sum \exp\left(W_j^T x_i + b_i\right)} \tag{5}$$

c. Parameters update by the gradient descent method

The cost function of the CNN network has many forms, such as squared error function, cross entropy, and so on. The general classification problem uses the form of cross entropy with the loss expression of the system as:

$$\mathrm{C} = -\frac{1}{n}\sum\nolimits_x [y \ln a + (1 - y)\ln(1 - a)] \tag{6}$$

where C represents the cost function, x represents the sample size, y represents the actual value, a represents the output value, and n represents the sample size. Backpropagation is needed to update the initial parameters θ by the gradient descent method. As the number of iterations increases, the return value of the cost function becomes smaller and smaller, meaning that the current output gradually approaches the target output. The number of iterations was decided when the training error is small enough. The training process is shown in Figure 7.

In practical applications, a large number of samples are usually difficult to obtain, which often leads to over fitting. This study used the rectified linear unit (ReLU) and the Dropout method to improve the imbalance between the high dimensionality of spectral data and small sample size. ReLU can enhance the expression ability of model and accel-

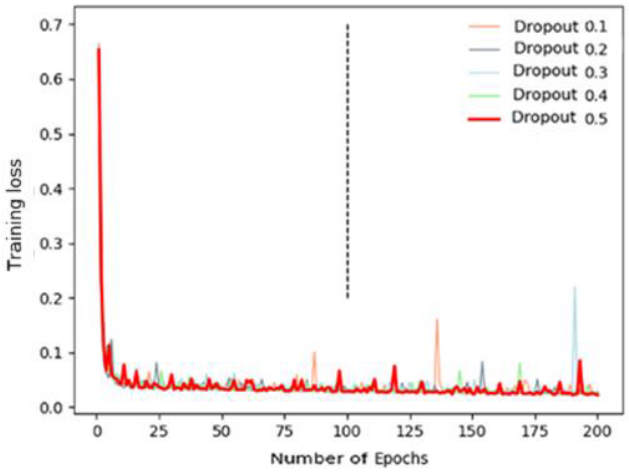

FIGURE 8. The training losses with dropout parameters 0.1, 0.2, 0.3, 0.4 and 0.5.

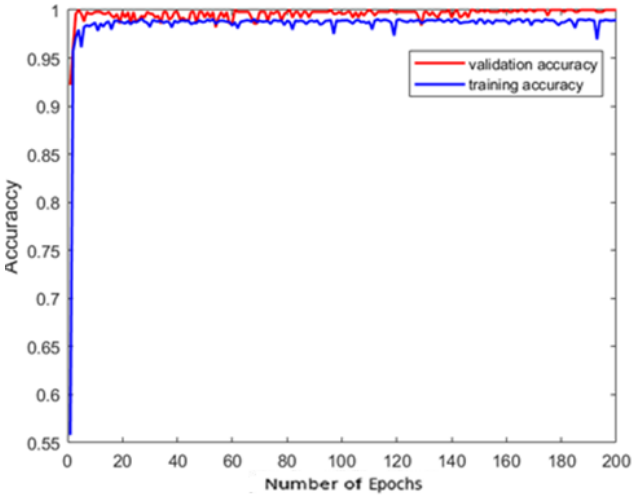

FIGURE 9. The training losses and accuracy results.

erate the convergence. The Dropout method randomly discards some model parameters and sets some hidden neurons to zero. It also establishes different network models in different training iterations. Therefore, its features are suitable for high-dimensional spectral data input and can improve the robustness of the model. During the training process, 80% of the training samples were used to learn the weighting parameters of each neuron, and the remaining 20% were used as a verification set to evaluate the performance of the network and guide the correct architecture design. When optimizing the model, we focused on adjusting the number of convolution kernels, the size of the convolution kernel and the number of neurons in the fully connected layer. We then made adjustments according to the convergence rate of the model.

Adding the Dropout layer doubles the training time of a network. Therefore, the network structure only adopted the Dropout strategy at the fully connected layers. The selection of Dropout parameters in model training has a great influence on the training result. Therefore, five parameters in the range of 0.1-0.5 were tested in the training process, as shown in Figure 8. It is found that the classification model is optimal when Dropout is set as 0.5. The overall convergence is faster when the Dropout is 0.5 as well. The training is optimal after 100 iterations.

The trend of training error and classification accuracy with the number of iterations is shown in Figure 9. It is observed that the classification accuracy of the training set is high and continuously improved. The effect of the test set is also ideal, so the optimal classification model is finally determined. In general, training accuracy is better than validation accuracy. From Figure 9 we can see validation accuracy was better than training accuracy, which is because Dropout layer was added. A percentage of the features were set to zero (dropout) during training, while all features were used during validation. This led to higher validation accuracies.

Based on the above analysis, the specific network structure parameters are shown in Table 3, with I1 as the input layer, C2, C3, C5, C6 and C7 as the convolution layers, P4 and P8 as the largest pooling layers, F9 as the fully connected layer, and O10 as the output layer of the convolutional neural network. Input layer I1 was set as 3×1 after principal component analysis, and the decisive dimension of the input was 5. The size of the convolution kernel was set as 3×1 because one-dimensional CNN filters were used.

B. THE TEST RESULT OF CNN

Table 4 and Figure 10 show the CNN detection results and chemical method results. It can be seen from Table 4 that the detected cold-stressed plant pixels of different varieties of corn seedlings were significantly different when using the CNN detection model. And chemical method results of different kinds of corn reed are different too. According to the research conclusion from Enders et al. [39], where the percentage of necrotic tissue was assessed for 40 genotypes after 7°C stress at day 11, some genotypes had a significant increase in tissue necrosis rate compared to the controls. Among the five genotypes used in this study, tissue necrosis rates of four (W22, B73, PH207 and M17) were given in Enders et al. (2019). From Figure 10 we can see the detected cold damage results W22 (41.83%), BxM (35%), B73 (25.6%), PH207 (20%), Mo17 (14%) in this study had high correlation confidence with the ranking given by chemical method in Tara A. Enders et.al [39]. The correlation confidence between cold damage detection results of CNN and results from chemical method are 0.8219.

The CNN model effectively overcomes the shortcomings of BP network that are easy to fall into local optimum and long training time due to random initialization weight parameters, and can better solve practical problems such as high dimensionality, nonlinearity and local mini-

TABLE 3. The structure of the CNN model.

Corn seedling freeze damage recognition model		Architecture configuration
Input layer (I1)		64, 3*1
One-dimensional convolution layer Conve2(C2)	ReLU	**Filters**(The number of convolution kernels, the dimensions of the output): 64 **Kernel size** (Airspace window length of convolution kernel): 3*1
One-dimensional convolution layer Conve3(C3)	ReLU	**Filters**(The number of convolution kernels, the dimensions of the output): 64 **Kernel size** (Airspace window length of convolution kernel): 3*1
Pooling1	(P4)	Pool size: 3*1
One-dimensional convolution layer Conve5 (C5)	ReLU	**Filters**(The number of convolution kernels, the dimensions of the output): 128 **Kernel size** (Airspace window length of convolution kernel): 3*1
One-dimensional convolution layer Conve6 (C6)	ReLU	**Filters**(The number of convolution kernels, the dimensions of the output) :128 **Kernel size** (Airspace window length of convolution kernel): 3*1
One-dimensional convolution layer Conve7 (C7)	ReLU	**Filters**(The number of convolution kernels, the dimensions of the output): 128 **Kernel size** (Airspace window length of convolution kernel): 3*1
Pooling8(P8)		**Pool size**: 3*1
Fully connected layer (F9)	Sigmoid	**Units** (Output dimension): 1
Classified output (O10)		2

TABLE 4. The results of detection of cold damage of corn seeding using CNN model and chemical method.

Cultivars	Cold damage Results of CNN (%)	Cold damage Results of chemical method (%)
W22	41.8	17
BxM	35.0	N/A
B73	25.6	14
PH207	20	13.5
Mo17	14	12

mum points. It effectively avoids the occurrence of over-learning and under-learning. It can be seen that the performance of the CNN is stable and reliable in practical applications.

Our goal was to provide a basis for work towards maximizing the ability of maize to withstand and recover from early season cold stress events. Future study based on hyperspectral images still need to do more work.

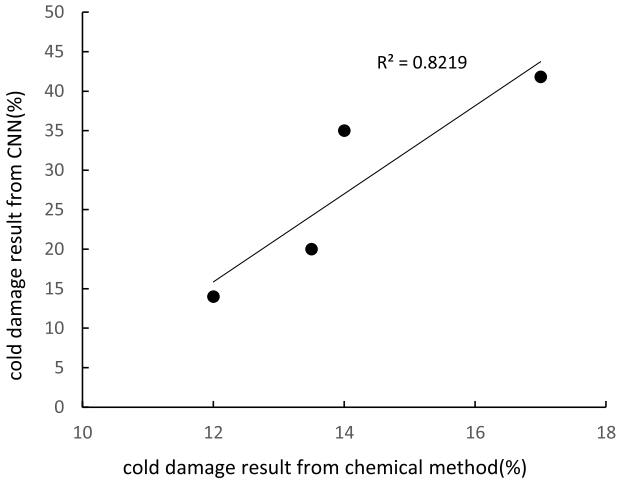

FIGURE 10. The comparing result of CNN and chemical method.

Hyperspectral image-based phenotyping methods can provide a more in-depth analysis of cold stress responses in maize.

V. CONCLUSION

Since the development of convolution neural networks, the high performance of algorithms has attracted the attention of scholars. At the same time, the effective identification of crop diseases is the need for smart agriculture development, but the traditional recognition model based on artificially designed features has lower accuracy and it is stable. Based on these problems, this paper uses CNN to design five varieties of corn seedling cold damage recognition model, detailing hyperspectral image pre-processing method, sample extraction method, and deep convolution networks. Different network structures are established corresponding to different input data in the whole process, and the segmentation result is obtained. In the case of a small sample of corn seedling cold damage, a convolution neural network is applied to the corn cold damage detection model, and the structure of the CNN model was constructed. The influence of the weight distribution characteristics, activation function and different initialization methods of the CNN is analyzed. By combining with the Dropout strategy to enhance the features, the over-fitting problem and the negative impact of network depth on the pre-training effect are solved. The model solves the defect of random initialization weight. Finally, under the small sample of corn seedling disease, the effectiveness of the pre-training method is verified, and CNN detected the best effects of different types of corn seedlings W22 (41.8%), BxM (35%), B73 (25.6%), PH207 (20%), Mo17 (14%) which had high correlation coefficient with the cold damage detection result obtained from chemical method. The next work will introduce hyperspectral image dimension features, extract the texture characteristics of crop disease tissue structure, and joint models with spectral dimension information to further improve the classification performance of the model.

REFERENCES

[1] C. Aguilera, C. M. Stirling, and S. P. Long, "Genotypic variation within Zea mays for susceptibility to and rate of recovery from chill-induced photoinhibition of photosynthesis," *Physiolo. Plantarum*, vol. 106, no. 4, pp. 429–436, Feb. 2002.

[2] C. M. Andorf, E. K. Cannon, J. L. Portwood, J. M. Gardiner, L. C. Harper, M. L. Schaeffer, B. L. Braun, D. A. Campbell, A. G. Vinnakota, V. V. Sribalusu, M. Huerta, K. T. Cho, K. Wimalanathan, J. D. Richter, E. D. Mauch, B. S. Rao, S. M. Birkett, T. Z. Sen, and C. J. Lawrence-Dill, "MaizeGDB update: New tools, data and interface for the maize model organism database," *Nucleic Acids Res.*, vol. 44, pp. D1195–D1201, Jan. 2016.

[3] R. Armonienė, F. Odilbekov, V. Vivekanand, and A. Chawade, "Affordable imaging lab for noninvasive analysis of biomass and early vigour in cereal crops," *Biomed Res. Int.*, Apr. 2018. Art. no. 5713158. doi: 10.1155/2018/5713158.

[4] M. A. Gehan, N. Fahlgren, A. Abbasi, J. C. Berry, S. T. Callen, L. Chavez, A. N. Doust, M. J. Feldman, K. B. Gilbert, J. G. Hodge, J. S. Hoyer, A. Lin, S. Liu, C. Lizárraga, A. Lorence, M. Miller, E. Platon, M. Tessman, and T. Sax, "PlantCV V2: Image analysis software for high-throughput plant phenotyping," *PeerJ*, vol. 5, Dec. 2017, Art. no. e4088. doi: 10.7717/peerj.4088.

[5] P. Revilla, V. M. Rodríguez, A. Ordás, R. Rincent, A. Charcosset, C. Giauffret, A. E. Melchinger, C.-C. Schöne, E. Bauere, T. Altmannf, D. Brunelg, J. Moreno-Gonzálezh, L. Campoh, M. Ouzunovai, J. Labordei, Á. Álvarez, J. I. R. de Galarretak, and R. A. Malvar, "Cold tolerance in two large maize inbred panels adapted to European climates," *Crop Sci.*, vol. 54, pp. 1981–1991, Jun. 2014.

[6] V. M. Rodríguez, A. Butrón, M. O. A. Rady, P. Soengas, and P. Revilla, "Identification of quantitative trait loci involved in the response to cold stress in maize (Zea mays L.)," *Mol. Breeding*, vol. 33, no. 2, pp. 363–371, Feb. 2014.

[7] B. Sánchez, A. Rasmussen, and J. R Porter, "Temperatures and the growth and development of maize and rice: A review," *Glob Chang Biol.*, vol. 20, no. 2, pp. 408–417, Feb. 2013.

[8] X. Zhang, H. Chen, and Y. Zheng, "Monitoring the freezing injury of winter wheat by remote sensing," *J. Nanjing Inst. Meteorol.*, vol. 29, no. 1, pp. 94–100, Jan. 2006.

[9] H. Kerdiles, M. Grondona, R. Rodriguez, and B. Seguin, "Frost mapping using NOAA AVHRR data in the Pampean region, Argentina," *Agricult. Forest Meteorol.*, vol. 79, pp. 157–182, Apr. 1996.

[10] J. C. Jiménez-Muñoz and J. A. Sobrino, "A generalized single-channel method for retrieving land surface temperature from remote sensing data," *J. Geophys. Res.*, vol. 108, noD22, pp. ACL2-1–ACL2-9, Nov. 2003.

[11] C. Jurgens, " The modified normalized difference vegetation index (mNDVI) a new index to determine frost damages in agriculture based on Landsat TM data," *Int. J. Remote Sens.*, vol. 18, no. 17, pp. 3583–3594, 1997.

[12] M.-C. Feng, W.-De Yang, L.-L. Cao, and G.-W. Ding, "Monitoring winter wheat freeze injury using multi-temporal MODIS data," *Agricult. Sci. China*, vol. 8, no. 9, pp. 1053–1062, Sep. 2009.

[13] P. Romanov, "Satellite-derived information on snow cover for agriculture applications in Ukraine," in *NATO Science for Peace and Security Series C: Environmental Security*. Oct. 2011, pp. 81–91.

[14] L. Jun-Ling, Y. Wei-Dong, Z. Hong, and G. Qi-Le, "Study on hyperspectral sensitivity index of winter wheat after freeze injury at mid-winter period," *Chin. J. Agro Meteorol.*, vol. 35, no. 6, pp. 708–716, Apr. 2014.

[15] W. Chenyang, *Early Diagnosis of Winter Wheat Night Frost Damage Based on Hyperspectral Remote Sensing Technology*. Nanjing, China: Nanjing Agriculture Univ., 2013.

[16] H. F. Wang, J. H. Wang, Y. Y. Dong, X. H. Gu, and Z. G. Huo, "Monitoring freeze stress levels on winter wheat from hyperspectral reflectance data using principal component analysis," *Spectrosc. Spectral Anal.*, vol. 34, no. 5, pp. 1357–1361, May. 2014.

[17] *State Agriculture Overview*. Accessed: Jun. 2019. [Online]. Available: https://www.nass.usda.gov/Quick_Stats/Ag_Overview/stateOverview.php?state=minnesota

[18] J. Yang, Q. Guo, and W. Tao, "Effects of freezing damage of maize seedling on its growth and development and preventive measures," *Ningxia Agricult. Forestry Sci. Technol.*, vol. .4, pp. 21–22, Aug. 2006.

[19] S. Sun, Y. Zhou, J. Chen, J. Shi, H. Zhao, H. Zhao, W. Song, M. Zhang, Y. Cui, X. Dong, and H. Liu, "Extensive intraspecific gene order and gene structural variations between Mo17 and other maize genomes," *Nature Genet.*, vol. 50, no. 9, pp. 1289–1295, Jul. 2018.

[20] H. Shuangping, S. Chao, Q. Long, X. Ma, and W. Wang, "Rice panicle blast identification method based on deep convolution neural network," *Trans. Chin. Soc. Agricult. Eng.*, vol. 33, no. 20, pp. 169–176, Oct. 2017.

[21] L. Tianyu and F. Quan, "Detecting grape leaves based on convolutional neural network," *J. Northwest Univ. (Natural Sci. Edition)*, vol. 47, no. 4, pp. 505–512, Apr. 2017.

[22] L. Qing, T. Xianlun, and Z. Na, "Structure optimized convolution neural network based on unsupervised pre-training," *Adv. Eng. Sci.*, vol. 49, no. Supp. 2, pp. 210–215, Jun. 2017.

[23] T. Wenxue, "Research on methods for crop lesion image processing and disease recognition with machine learning," Dept. Comput. Sci. Technol., Beijing Univ. Technol., Beijing, China, 2016.

[24] W. Huifang, J. Wang, Q. Wang, N. Miao, W. Huang, H. Feng, and Y. Dong, "Hyperspectral characteristics of winter wheat under freeze injury stress and LWC inversion model," presented at the 1st Int. Conf. Agro-Geomform. (Agro-Geoinformatics), 2012. doi: 10.1109/Agro-Geoinformatics.2012.6311627.

[25] Z. Zhaoyong, L. Yu, S. Dong, Z. Haihui, H. Dongjian, and C. Yang, "Detection of moldy core in apples and its symptom types using transmittance spectroscopy," *Int. J. Agricult. Biol. Eng.*, vol. 9, no. 6, pp. 148–155, Nov. 2016.

[26] P. Leiqing, Q. Zhang, W. Zhang, Y. Sun, P. Hu, and K. Tu, "Detection of cold injury in peaches by hyperspectral reflectance imaging and artificial neural network," *Food Chem.*, vol. 192, pp. 134–141, Feb. 2016.

[27] D. Lorente, N. Aleixos, J. Gómez-Sanchis, S. Cubero, O. L. García-Navarrete, and J. Blasco, "Recent advances and applications of hyperspectral imaging for fruit and vegetable quality assessment," *Food Bioprocess Technol.*, vol. 5, no. 4, pp. 1121–1142, Nov. 2011.

[28] F.-Y. Wang, K.-R. Wang, S.-K. Li, S. Gao, C.-H. Xiao, B. Chen, J.-L. Chen, Y.-L. Lü, and W. Y. Diao, "Estimation of canopy leaf nitrogen status using imaging spectrometer and digital camera in cotton," *Acta Agronomica Sinica*, vol. 37, no. 6, pp. 1039–1048, Jun. 2011.

[29] J. Luo, W. Huang, L. Yuan, C. Zhao, S. Du, J. Zhang, and J. Zhao, "Evaluation of spectral indices and continuous wavelet analysis to quantify aphid infestation in wheat," *Precis. Agricult.*, vol. 14, no. 2, pp. 151–161, Apr. 2013.

[30] J. Zhang, R. Pu, W. Huang, L. Yuan, L. Luo, and J. Wang, "Using in-situ hyperspectral data for detecting and discriminating yellow rust disease from nutrient stresses," *Field Crops Res.*, vol. 134, no. 12, pp. 165–174, Aug. 2012.

[31] H. L. Jin, L. Li, and J.-H. Cheng, "Rapid and non-destructive determination of moisture content of peanut kernels using hyperspectral imaging technique," *Food Anal. Methods*, vol. 8, no. 10, pp. 2524–2532, Mar. 2015.

[32] X. Glorot, A. Bordes, and Y. Bengio, "Deep sparse rectifier neural networks," in *Proc. 14th Int. Conf. Artif. Intell. Statist.*, Fort Lauderdale, FL, USA, vol. 15, 2011, pp. 315–323. [Online]. Available: http://proceedings.mlr.press/v15/glorot11a.html

[33] K. Jarrett, K. Kavukcuoglu, M. Ranzato, and Y. LeCun, "What is the best multi-stage architecture for object recognition?" in *Proc. IEEE 12th Int. Conf. Comput. Vis.*, Sep./Oct. 2009, pp. 2146–2153. doi: 10.1109/ICCV.2009.5459469.

[34] V. Nair and G. E. Hinton, "Rectified linear units improve restricted Boltzmann machines," in *Proc. 27th Int. Conf. Int. Conf. Mach. Learn.* Madison, WI, USA: Omnipress, 2010, pp. 807–814. [Online]. Available: http://dl.acm.org/citation.cfm?id=3104322.3104425

[35] D. Wu, H. Shi, S. Wang, Y. He, Y. Bao, and K. Liu, "Rapid prediction of moisture content of dehydrated prawns using online hyperspectral imaging system," *Analytica Chim. Acta*, vol. 726, no. 9, pp. 57–66, May 2012.

[36] P. Vincent, H. Larochelle, I. Lajoie, Y. Bengio, and P.-A. Manzagol, "Stacked denoising autoencoders: Learning useful representationsina deep network with a local denoising criterion," *J. Mach. Learn. Res.*, vol. 11, no. 12, pp. 3371–3408, Dec. 2010.

[37] D. Wu, D.-W. Sun, and Y. He, "Application of long-wave near infrared hyperspectral imaging for measurement of color distribution in salmon fillet," *Innov. Food Sci. Emerg. Technol.*, vol. 16, no. 39, pp. 361–372, Oct. 2012.

[38] X.-Y. Niu, L.-M. Shao, Z.-L. Zhao, and X.-Y. Zhang, "Nondestructive discrimination of strawberry varieties by NIR and BP-ANN," *Spectrosc. Spectral Anal.*, vol. 32, no. 8, pp. 2095–2099, Aug. 2012.
[39] T. A. Enders, S. S. Dennis, J. Oakland, S. T. Callen, Ma. A. Gehan, N. D. Miller, E. P. Spalding, N. M. Springer, and C. D. Hirsch, "Classifying cold-stress responses of inbred maize seedlings using RGB imaging," *Plant Direct*, vol. 3, no. 1, pp. 1–11, Art. no. e00104.

WEI YANG received the B.S. degree in electrical engineering and the Ph.D. degree in agricultural engineering from China Agricultural University, in 2003 and 2009, respectively.

Since 2014, she has been an Associate Professor with China Agricultural University, Beijing, China. Her research interests include remote sensing applications for precision agriculture, hyperspectral and multispectral imaging, computer vision, and machine learning. She has been a member of the American Society of Agricultural and Biological Engineering for eight years. From 2003 to 2009, she received the Graduate School Fellowship that supported her Ph.D. research.

CE YANG received the B.S. degree in electrical engineering and the M.S. degree in agricultural engineering from China Agricultural University, in 2007 and 2009, respectively, and the M.S. degrees in agricultural engineering and computer science from the University of Florida, in 2013 and 2014, respectively.

Since 2014, she has been an Assistant Professor with the University of Minnesota, Twin Cities, MN, USA. Her research interests span remote sensing, deep learning, and machine learning to solve agricultural problems, such as plant stress detection, crop yield detection, and nitrogen management using advanced tools and techniques.

Dr. Yang has been a member of the American Society of Agricultural and Biological Engineering for eight years. From 2009 to 2014, she received the Graduate School Fellowship that supported her Ph.D. research.

ZIYUAN HAO received the B.S. degree in electrical engineering from China Agricultural University, in 2017. She is currently pursuing the Ph.D. degree in agricultural engineering.

Her research interests include remote sensing and deep learning used on crop yield detection.

Ms. Hao was a recipient of the Graduate School Fellowship, from 2017 to 2019.

CHUANQI XIE received the Ph.D. degree in bio systems engineering from Zhejiang University, in 2015.

From 2014 to 2015, he was an Exchange Ph.D. Student/Visiting Research Scholar with the Department of Agricultural and Biological Engineering, University of Florida. From 2015 to 2018, he was a Postdoctoral Associate with the Department of Bioproducts and Biosystems engineering, University of Minnesota (Twin Cities). He is currently a Lecturer with the Department of Food Science and Engineering, East China University of Science and Technology. His research interests include agricultural engineering, food engineering, hyperspectral imaging, and so on.

MINZAN LI received the B.S. degree in mechanical engineering and the M.S. degree in mechanical engineering from Beijing Agricultural Mechanization Institute, in 1982 and 1991, respectively, and the Ph.D. degree from the National Tokyo University of Agriculture and Technology, in 2000.

Since 2002, he has been a Professor with China Agricultural University, Beijing, China. He is an expert in spectroscopy and spectral analysis. His research interests include remote sensing, agricultural engineering, and hyperspectral imaging. He has been a member of the American Society of Agricultural and Biological Engineering for many years.